Applied Energy 185 (2017) 440–451

Contents lists available at ScienceDirect

Applied Energy

journal homepage: www.elsevier.com/locate/apenergy

Disturbance analysis of a free-piston engine generator using a validated fast-response numerical model

Boru Jia [a,b], Andrew Smallbone [a,*], Rikard Mikalsen [a], Huihua Feng [b], Zhengxing Zuo [b], Anthony Paul Roskilly [a]

[a] Sir Joseph Swan Centre for Energy Research, Newcastle University, Newcastle upon Tyne NE1 7RU, UK
[b] School of Mechanical Engineering, Beijing Institute of Technology, Beijing 100081, China

HIGHLIGHTS

- Different types of system disturbance with specific occurring times were identified.
- The influence of each disturbance on the FPE system was characterised.
- Technically feasible control variables were identified.
- Control variable coupled with a system controller design was presented.

ARTICLE INFO

Article history:
Received 6 May 2016
Received in revised form 6 October 2016
Accepted 16 October 2016
Available online 10 November 2016

Keywords:
Free-piston engine
Generator
Disturbance
Numerical model

ABSTRACT

In this paper, a fast-response numerical model was used to investigate potential disturbances to a free-piston engine generator (FPEG), i.e. engine cycle-to-cycle variations, misfire and immediate electric load change. During the engine operation, there could be one disturbance taking place or several disturbances take place simultaneously. By identifying different types of system disturbance with specific occurring times, the influence on the system was characterised. It was found that a step change of electric load would induce a corresponding top dead centre (TDC) step change. Low variations on piston TDC are observed when cycle-to-cycle variations take place. When unsuccessful ignition occurs, the engine will stop after one oscillation cycle. Reducing the electric load after misfire would cause more oscillation cycles and require a restart of the engine. Technically feasible control variables were identified and coupled with a PI feedback controller design to minimise the impact of each kind of disturbance, a design which could be used in future FPE control system designs. The controller performance was seen to be satisfactory for the electric load step change, and the piston TDC was controlled to back to the set point in 0.5 s.

1. Introduction

The free-piston engine (FPE) is a linear engine conversion device that compromises a linear combustion engine coupled with a load system [1–4]. The reported effective efficiency of FPE is up to 46% at a power level of 23 kW with promising emission results [5]. Due to the lack of crankshaft mechanism, the complexity of the engine is significantly reduced, and the piston assembly is the only significant moving part. This gives a number of advantages upon conventional engines such us reduced frictional losses, higher power-volume ratio, and multi fuel/combustion mode possibility [6–8]. Typical modern applications of the FPE concept have been proposed with electric load or hydraulic load, and are now being investigated worldwide [9–17]. However, the piston movement for FPE is not limited by the crankshaft-connection rod system, it moves freely between its dead centres. Hence, the piston dynamics is prone to be influenced by disturbances from both internal and external sources [18], which could induce to unstable operation, even engine misfire. As a result, the identification and control of disturbance to FPE are of significant importance to the further development of control system, while there has not been detailed research report this specific area.

Mikalson and Roskilly investigated the FPE control variables and disturbances using a full-cycle simulation model [19,20]. The

* Corresponding author.
E-mail addresses: b.jia@newcastle.ac.uk (B. Jia), andrew.smallbone@ncl.ac.uk (A. Smallbone).

http://dx.doi.org/10.1016/j.apenergy.2016.10.143
0306-2619/

Nomenclature

A	piston surface area (m^2)	k_v	coefficient of the load force (N/m s^{-1})
C	controller transfer function	k	spring constant
C_1	constant	L_c	clearance length (m)
C_2	constant	L_s	length of half stroke (m)
C_v	heat capacity at constant volume (J/m^3 K)	m	moving mass of the mover with the pistons (kg)
CR	set geometric compression ratio	m_f	injected fuel amount (kg)
c	damping coefficient	p_0	ambient pressure (Pa)
c_c	critical damping coefficient	R	reference input for the control loop
E	control error	U	control variable
F	excitation force (N)	V_0	cylinder volume at the beginning of the compression stroke (m^3)
G	transfer function of the FPEG system	x	mover displacement (m)
H_u	low heating value of the fuel with the combustion efficiency (J/kg);	x_{TDC}	target top dead centre (m)
H_n	engine speed (Hz)	Y	system output
K_p	proportional gain	γ	heat capacity ratio
K_i	integral gain	ω	angular natural frequency (rad/s)
K_d	derivative gain	η_c	random combustion efficiency

load force from the electric machine was identified as a disturbance to the FPE, and carried a high influence on both the engine speed and dead centre positions [19]. Variations in the injected fuel mass were found to affect the indicated mean effective pressure and peak in-cylinder pressure, and the variations were observed to be higher for the FPE than for the conventional engine. This was reported to be due to the variations in the combustion energy from cycle 1 which would influence the compression ratio for the cycles 2, 3, 4, etc. The combination of variations in both compression ratio and injected fuel mass would be expected to lead significantly higher peak cylinder pressure variations in the FPEG technologies [20].

A high-speed free-piston diesel engine was developed by Johansen et al. aimed at marine applications as an alternative to both gas turbines and traditional diesel engines [21–23]. Timing inaccuracies were reported to lead to disturbances on the piston force balance, furthermore the piston motion would vary from cycle-to-cycle. A slightly late opening of the exhaust valve would induce a higher pressure in the combustion chamber and result in an undesired increase in the stroke length [21]. Cycle-to-cycle variations would also induce to pressure disturbance in the intake and exhaust manifold. The variability in the stroke was demonstrated to be controlled within 2 mm out of a stroke of about 200 mm [21].

The free-piston engine generator (FPEG) prototype developed by Beijing Institute of Technology was reported to misfire every one to two cycles, with severe cycle-to-cycle variations [24]. The possible sources of the variations and unstable operation were considered to be (1) the air/fuel mixture formation might vary from cycle to cycle in cold engine conditions, (2) the spark and initial flame propagation could have cyclic variations as normal SI engines, (3) the unstable combustion could lead to an undesired piston profile and then influence the heat release process in the next cycle [24].

The FPEG prototype developed by Toyota Central R&D Labs Inc. was a single piston type with a gas rebound device [25,26]. A power generation experiment was carried out, and results demonstrated that the prototype operated stably for a long period of time [26]. Pre-ignition was found to occur during the test, and the cylinder pressure in the combustion chamber increased earlier than the spark timing. As a result, the oscillation frequency was disturbed, and temporary unstable operation was observed. With the help of the designed feedback control system, the system was reported to recover from the unstable state in less than 1 s [26].

This paper aims to analyse the possible disturbances to the FPEG prototype using a fast-response numerical model, and reject the disturbances with feasible controller. By identifying different types of system disturbance with specific occurring times, the influence on the system can be characterised. Technically feasible control variables were identified and coupled with a system controller design to minimise the impact of each kind of disturbance, a design which can be used in future FPE control system designs.

2. FPEG System simulation

2.1. FPEG configuration

The designed spark-ignited FPEG prototype is illustrated in Fig. 1. The system is compromised two opposing internal combustion engine, and a linear electric generator is placed in the middle of two cylinders. The engine is operated using a two-stroke gas exchange process, and the power stroke is controlled to take place alternately in each cylinder to drive the compression stroke in the opposite side. As a result, the mover reciprocates between its dead centres, and the generator converts this mechanical energy into electricity, which will be stored by an external load. More information about the prototype development approach can be found in elsewhere [27].

2.2. Fast-response numerical model description

The FPEG is commonly modelled using several differential equations to characterise the piston dynamics and simulate engine performance [7,14]. All the design parameters are coupled with each other in these models, making them overly complex to be used in the real-time control system as the differential equations are solved iteratively. As a result, assumptions are made to simplify the system, i.e. (a) energy consumed by the heat transfer to the cylinder walls and gas leakage through the piston rings are ignored; (b) the running cycle of FPEG is two adiabatic compression/expansion processes connected with a constant volume heat release process. The FPEG system is finally described by a forced mass-spring vibration system under external excitation, which is illustrated in Fig. 2. Details for the simplification and derivation can be found in our previous publications [28].

The simplified dynamic equation is expressed as:

$$m\ddot{x} + c\dot{x} + kx = F(t) \tag{1}$$

$$c = k_v \tag{2}$$

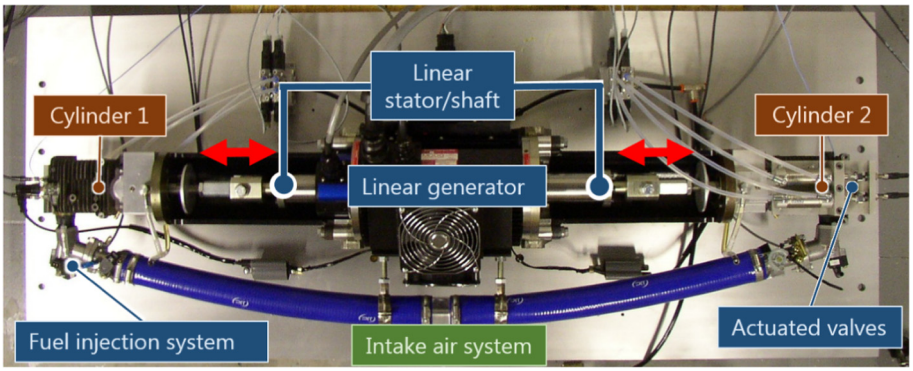

Fig. 1. Prototype configuration [27].

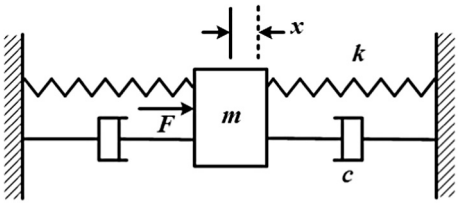

Fig. 2. Illustration of the analogous forced vibration system.

$$k = \frac{2\gamma p_0 A}{L_s} + \frac{m_f H_u \eta_c R \gamma}{C_v L_s^2 C R^{\gamma-1}} \tag{3}$$

$$F(t) = F_0 \sin \omega t \tag{4}$$

$$F_0 = \frac{4}{\pi} \frac{m_f H_u \eta_c R}{C R^{\gamma-1} L_s C_v} \tag{5}$$

where m is the moving mass of the mover with the pistons (unit: kg); x is the mover displacement (m); the constant c is the damping coefficient; the constant of proportionality k is the spring constant; k_v is the coefficient of the load force, and it varies with the load resistance; and $F(t)$ is the excitation force;γ is the heat capacity ratio; p_0 is the ambient pressure (Pa); A is the piston surface area (m^2); L_s is the length of half stroke (m); m_f is the injected fuel amount to the combustion chamber (kg); L_c is the length of the clearance (m); CR is the set geometric compression ratio, which is affected by the ignition timing due to the ideal constant volume heat release process; H_u is the low heating value of the fuel(J/kg); η_c is the combustion efficiency; C_v is the heat capacity at constant volume (J/m^3 K); V_0 is the cylinder volume at the beginning of the compression stroke (m^3).

The angular natural frequency ω of a FPEG is expressed by:

$$\omega = \sqrt{k/m} \tag{6}$$

The solution to Eq. (1) can be obtained according to vibration theory [29], and the piston displacement is then defined by:

$$x = -\frac{F_0 \cos \omega t}{c\omega} \tag{7}$$

2.3. Model validation and simulation results

The fast response model was validated with test data from a running prototype with a maximum stroke of 70 mm [28]. The simulated piston displacement was compared with the test data at the same operating condition, which is shown in Fig. 3. With the same input parameters, the simulation results of the piston dynamics show similar trends with the test results, and the tested

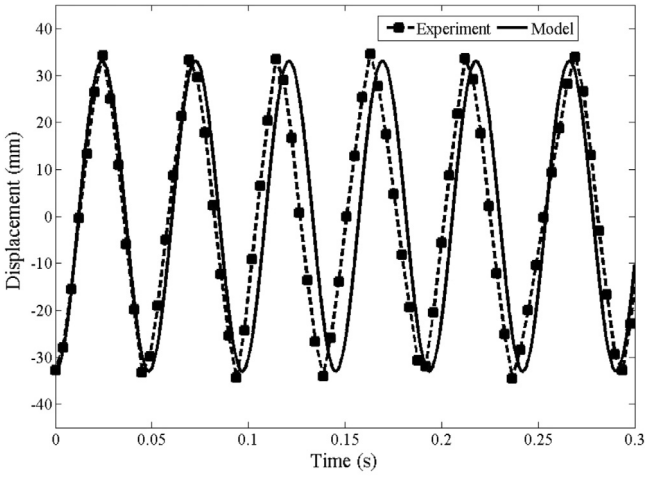

Fig. 3. Model validation results [28].

amplitudes are almost identical to the simulation. The fast-response numerical model is considered of acceptable accuracy to predict the experimentally observed piston dynamics. More information on the prototype used for model validation can be found elsewhere [2,3,6,7,24,28,30,31], and details for the method employed for model validation can be found in Ref. [28].

The fast-response numerical model was developed in Matlab/Simulink, calibrated using parameters and test data obtained from an operating FPEG prototype. The main design data of the prototype used in this paper are listed in Table 1. This prototype configuration is identical to the input parameters used in this model. During the steady operation, the fuel delivery and ignition systems are activated and the electrical discharge between the spark plug electrodes starts the combustion process close to the end of the compression stroke. The engine size is determined during the design process, which cannot be changed immediately during the operation. However, the electric load can make immediately changes during the generating process, the mode of the generator is able to be switched to a motor by the current vector motor control system. As shown in Fig. 4, the engine can be operated stably at

Table 1
Prototype parameters [27].

Parameter [unit]	Value
Bore [mm]	50
Maximum stroke [mm]	40
Moving mass [kg]	7
Coefficient of the load force [N/(m s^{-1})]	700

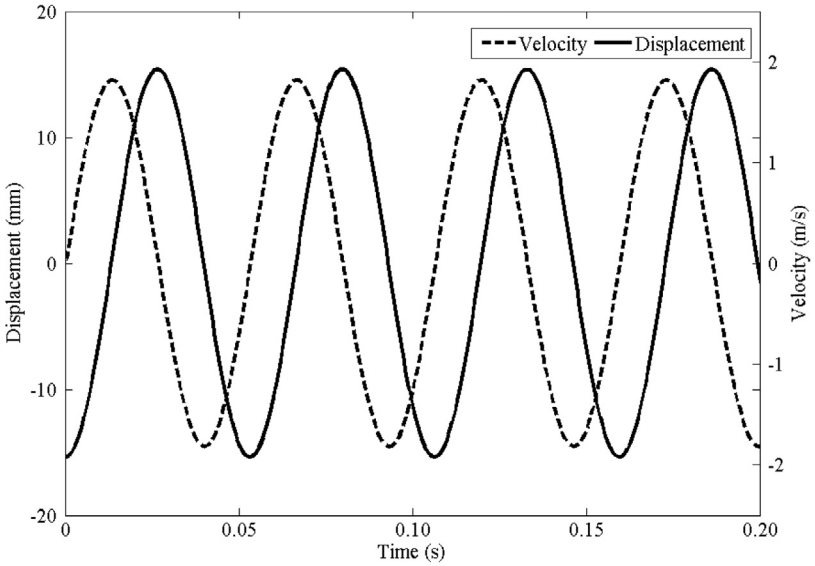

Fig. 4. Simulated piston dynamics during stable operation.

high load from the simulation, and the TDC achieved remains the same.

3. Potential system disturbance analysis

3.1. Introduction to disturbance

For conventional engines, the piston motion is imposed by the crankshaft mechanism, which defines the positions of the dead centres. However, for FPEs, the piston is not limited by the crankshaft mechanism, and its motion is only determined by the instantaneous sum of the forces acting on the mover. As illustrated in Fig. 5, any disturbance from either internal from the engine or external from the electric load may induce to variations in piston motion profile between consecutive cycles. The disturbances could result from an immediate change of electric load, engine cycle-to-cycle variations, or misfire.

A series of the two engine cycles mainly consist of four working processes: heat release, expansion, gas exchange and compression.

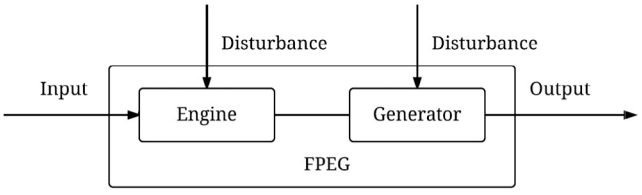

Fig. 5. Illustration of system disturbance.

As demonstrated in Fig. 6, the cycle-to-cycle combustion variations and engine misfire can only take place during the heat release process. However, the electric load change can occur anytime throughout out the operation. During the engine operation, there could be one disturbance taking place or several disturbances take place simultaneously. Several potential disturbance sources were identified and their differences on the engine performance will be discussed and characterised in the following section.

(1) Electric load change during expansion/gas exchange/compression/ heat release process.
(2) Cycle-to-cycle variations during heat release process.
(3) Unsuccessful ignition and thus no heat release process.
(4) Electric load change and cycle-to-cycle variations during heat release process.
(5) Electric load change and unsuccessful ignition during heat release process.

3.2. Influence to system performance

3.2.1. Electric load change

As an immediate electric load change can occur anytime during the engine operation, a simulation of immediate change at different working processes is undertaken to investigate the influence of the changing time to the piston dynamics. The engine is simulated to be operated at high load, and an immediate step change of the electric load is timed to occur at 0.5 s. Simulation results demonstrate that a corresponding changes in piston TDC is observed, and with different changing time, the TDC achieved dur-

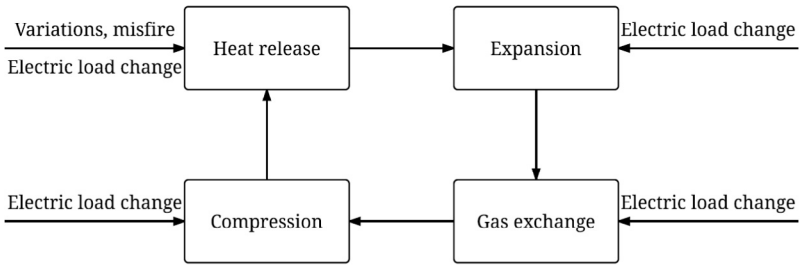

Fig. 6. Working processes with possible disturbances.

ing stable operation is identical. Fig. 7 demonstrates an example piston profile with a step decrease of the electric load by 15% (the coefficient of the load force in Table 1 decreases from 700 to 595). Fig. 8 shows an example of engine response to step increase of electric load by 5% (the coefficient of the load force in Table 1 increases from 700 to 735).

3.2.2. Cycle-to-cycle variations

Severe cycle-to-cycle variations have been described by experimental research articles in the operation of dual-piston FPEG [24]. The possible sources of these variations are considered to be a combination of a number of factors, i.e. intake/exhaust pressure variations in the manifold, combustion variations, air/fuel mixture formation variations [24]. As a result, the corresponding effective combustion efficiency, η_c varies. In this section, a random value of η_c from the range of m_f was employed used to investigate the influence of these variations on the engine performance. As shown in Fig. 9, low variations on the achieved piston TDC are observed. However, unlike conventional reciprocating engines, the unstable combustion in FPEs could affect the combustion process in the next cycle without the limitation of the crankshaft mechanism.

3.2.3. Unsuccessful ignition

During the operation of the FPEG, unsuccessful ignition could take place at any time. This problem could be caused by the unexpected failure of the spark plug/injector, or the power supply to the electronics, or poor air/fuel mixing, etc. When unsuccessful ignition happens, the excitation force changes to zero, as such FPEG system can be represented by a free vibration system with viscous damping, which is described by:

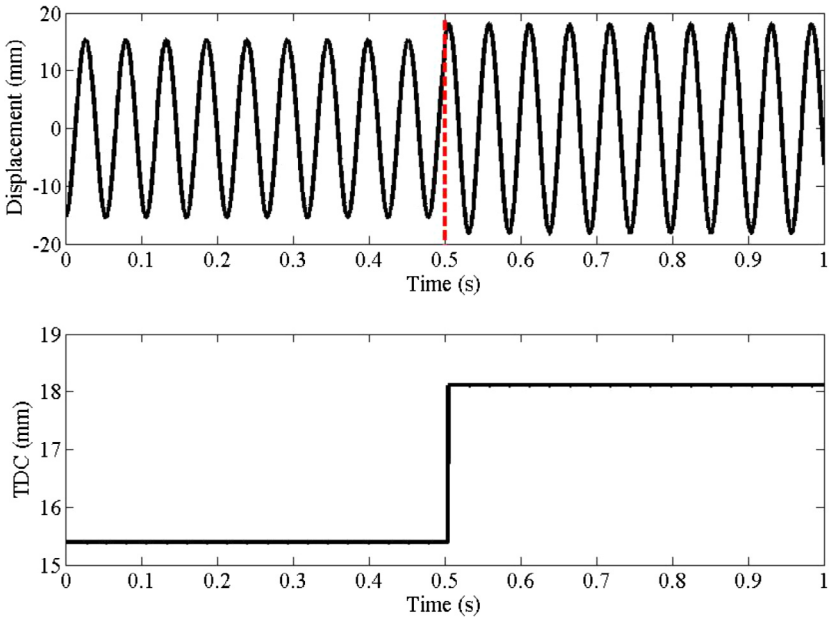

Fig. 7. Piston profile with step electric load decreases by 15%.

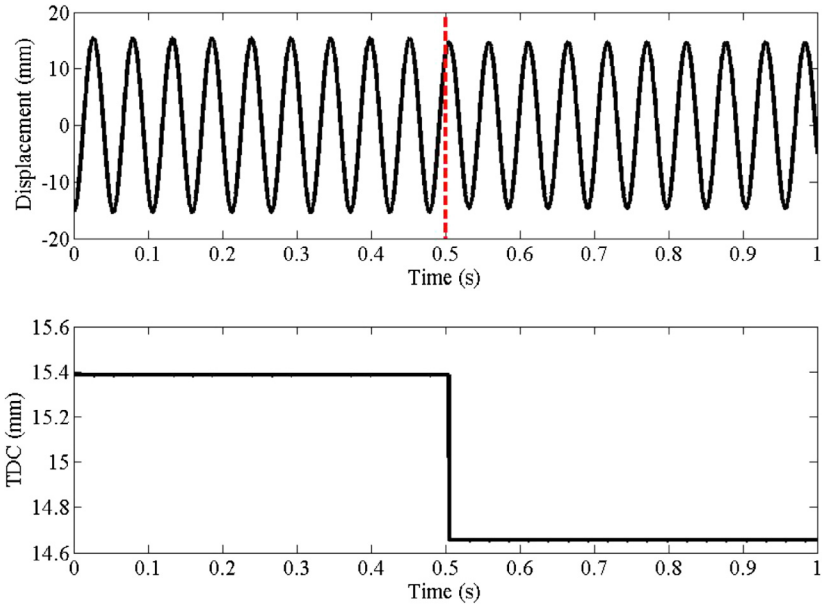

Fig. 8. Piston profile with step electric load increases by 5%.

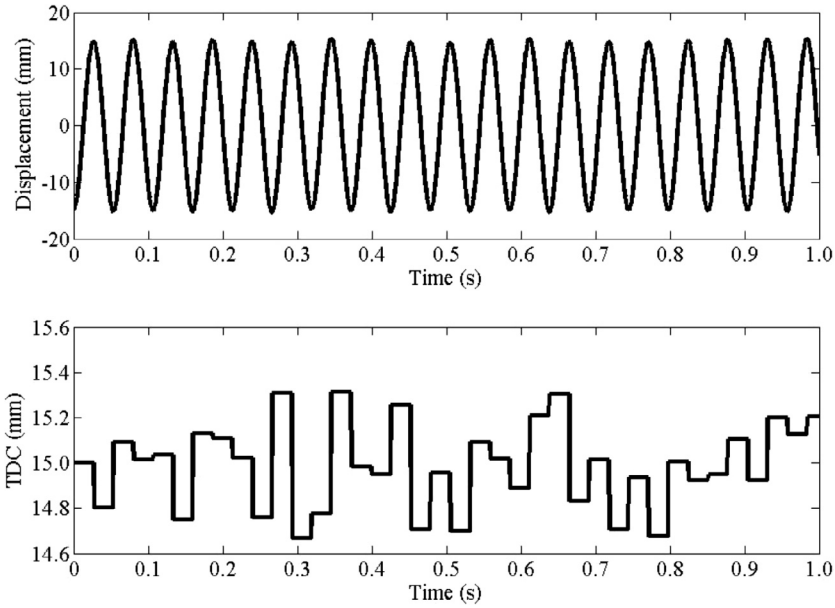

Fig. 9. Piston dynamics with cycle-to-cycle variations.

$$m\ddot{x} + c\dot{x} + kx = 0 \tag{8}$$

$$c = k_v \tag{9}$$

$$k = \frac{2\gamma p_0 A}{L_s} \tag{10}$$

As the damping coefficient is less than the critical damping coefficient c_c:

$$c_c = 2\sqrt{km} \tag{11}$$

The solution of Eq. (8) is underdamped according to the vibration theory [26], which can be expressed by:

$$x = e^{-ct/2m}(C_1 \sin \omega_d t + C_2 \cos \omega_d t) \tag{12}$$

where the value of C_1 equals to $\dot{x}/\omega$ at the time when unsuccessful ignition occurs, and C_2 is the value of x when unsuccessful ignition takes place. The damped natural frequency after misfire is then given by [29]:

$$\omega_d = \omega(1 - \zeta^2)^{1/2} \tag{13}$$

$$\zeta = c/c_c \tag{14}$$

After substituting the constant parameter to Eq. (12), the piston profile after an unsuccessful ignition is demonstrated in Fig. 10. It is overserved that when an unsuccessful ignition occurs in one operation cycle, the piston will be driven to the other side by the compressed air in the cylinder. Without the power force from the heat released by the gas mixture, the TDC achieved in the following cycle is significantly reduced, and cannot reach the required position for successful ignition. As a result, when unsuccessful ignition happens the engine stops after one oscillation cycle, and the piston stays in the middle of the stroke.

3.2.4. Electric load change with cycle-to-cycle variations

The data in Fig. 11 shows the influence of step electric load change along with cycle-to-cycle variations. At the time of 0.3 s, the electric load is controlled to decrease immediately by 15% (the coefficient of the load force in Table 1 decreases from 700 to 595). The model uses a random number generator $[0.95 - 1]$ to simulate cycle-to-cycle combustion variations. The piston TDC is observed to experience a step increase with small variations. Compared with the electric load change, the influence of the cycle-to-cycle variations to the piston TDC is minimal but could affect the on-going controller performance. As a result, both the electric load change and cycle-to-cycle variations are suggested to taken into account in the design process of the controller.

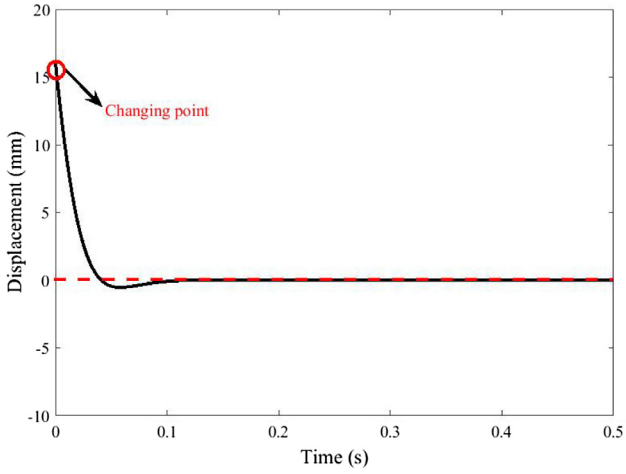

Fig. 10. Piston profile after misfire.

3.2.5. Unsuccessful ignition with electric load change

When an unsuccessful ignition occurs, the excitation source for the FPEG system is then reduced, and the system becomes a free vibration system with viscous damping. As the damping coefficient equals to the coefficient of the load force, when misfire happens, the piston profile is supposed to vary with the electric load. When the electric load is reduced to 0, the damping is eliminated, and the FPEG system can be described by:

$$m\ddot{x} + kx = 0 \tag{15}$$

The solution to Eq. (15) is then:

$$x = C_1 \sin \omega t + C_2 \cos \omega t \tag{16}$$

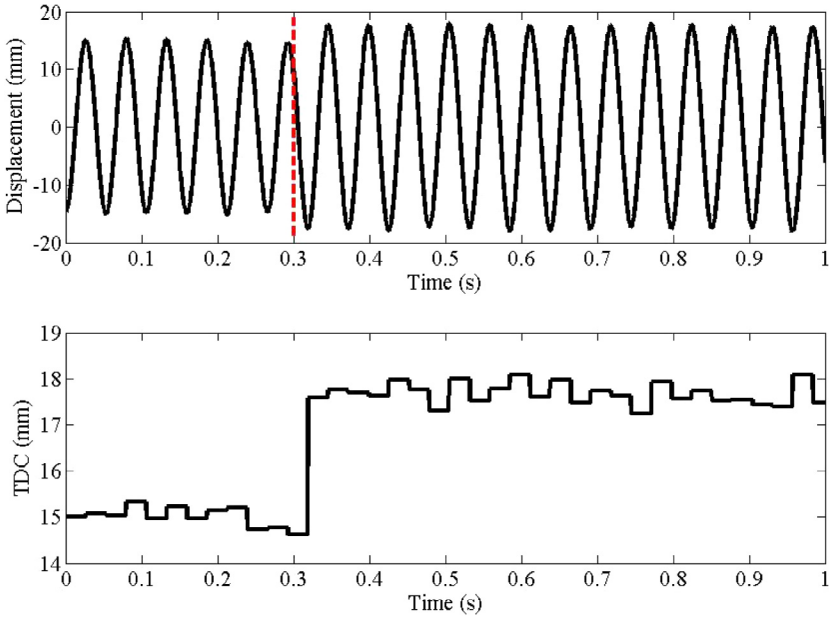

Fig. 11. Piston dynamics after electric load change along with variations.

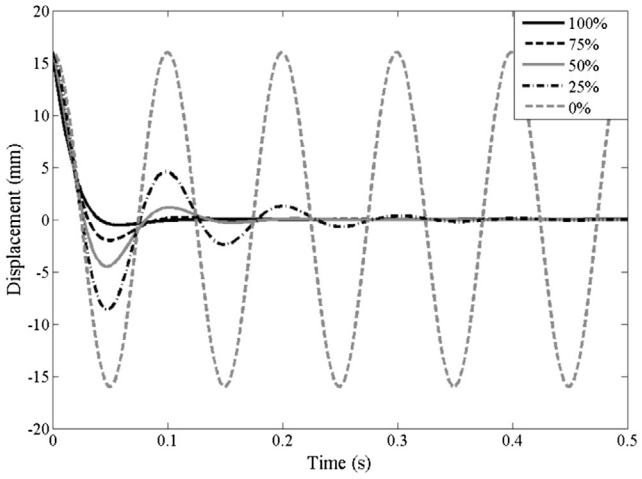

Fig. 12. Piston dynamics after misfire along with electric load change.

The data in Fig. 12 illustrates the piston trace after unsuccessful ignition along with immediate electric load change in percentage of the initial set value. The engine stops at the middle stroke after several oscillation cycles when disturbance occurs. With a lower electric load, more oscillation cycles are observed before the engine stops. It means that when unsuccessful ignition occurs, the engine will stop if the electric generator is still in operation, even at part load. If the electric load is reduced to zero, the sinusoidal oscillation of the mass will repeat continuously, and the TDC position remains affected. As a result, the recommended action is that the generator should be to switch off (or to a motor) immediately after unsuccessful ignition occurs to support the restart of the engine.

3.3. Unstable running analysis

As summarised in Table 2, for the various disturbances considered, the engine responses in three different ways, i.e. TDC step change, TDC small variations and stop. For FPEs, without the limitation of the crankshaft mechanism, the TDC must be controlled within tight limits to ensure sufficient compression and to avoid mechanical contact between piston and cylinder head [19]. When unsuccessful ignition occurs, the engine will stop and the linear generator is required to switch off or switch to a motor mode to restart the engine. For TDC step change or variations, an effective engine control system is required to recover the system and maintain the target TDC after disturbance occurs, which will be further investigated in the following section.

4. Disturbance control system

4.1. System input and output analysis

As the aim of control system is piston stable running, the piston is controlled to reach and maintain the target TDC, x_{TDC}. As a result, the TDC is selected as the system output, which can be calculated by:

$$x_{TDC} = \frac{F_0}{c\omega} = \frac{\frac{4m_f H_u R}{\pi C R^{\gamma-1} L_s C_v}}{k_v \sqrt{\frac{2\gamma p_0 A}{mL_s} + \frac{m_f H_u R \gamma}{mC_v L_s^2 C R^{\gamma-1}}}} \tag{17}$$

The engine speed, H_n (Hz) is a useful output sign for the observation of the engine operation, which is obtained by:

$$H_n = \sqrt{\frac{2\gamma p_0 A}{mL_s} + \frac{m_f H_u R \gamma}{mC_v L_s^2 C R^{\gamma-1}}} \Big/ 2\pi \tag{18}$$

Table 2
Summary of unstable running and potential control parameters.

	Electric load		Cycle-to-cycle variations	Unsuccessful ignition
	Step increase	Step decrease		
TDC response	Step decrease	Step increase	Variations	Stop

Table 3
Potential parameters influential to TDC.

	Input parameters		
	Engine size	Working conditions	Electric load
TDC	Piston area, A Half stroke length, L_s Moving mass, m	Injected fuel mass, m_f	Coefficient of the load force, k_v
Engine operating frequency (speed)	Piston area, A Half stroke length, L_s Moving mass, m	Injected fuel mass, m_f	–

From Eqs. (17) and (18), it is apparent that both the TDC and engine speed are influenced by various input parameters, which can be further selected as control variables. The potential control parameters are summarised in three categories, which are summarised in Table 3. The engine capacity is decided during the hardware design process, thus piston area, stroke length and moving mass are not considered as technically feasible real-time control inputs. As the changing of the load force is often considered as a disturbance [19,20], the injected fuel mass is selected as the main control variable in this paper. More discussions on the control objectives and control variables for the FPEG can be found in elsewhere [32].

Varying the amount of fuel injected will affect the amount of energy released in the combustion process. The data in Fig. 13 shows the effect of the injected fuel mass per cycle on engine operation performance using Eqs. (17) and (18). When the injected fuel mass changes from a wide range from −90% to 90%, i.e. without considering its physical feasibility, the TDC increases from 2 mm to 24 mm. The engine TDC is directly sensitive to the injected fuel mass amount, and small variations in the current engine can lead to significant changes in TDC and compression ratio. For an engine with a stroke length of 40 mm, as considered here, a TDC variation of ±1% of the stroke length would be equivalent to 0.4 mm and would produce a compression ratio variation of approximately ±1.0. However, the influence of the injected fuel mass on the engine speed is not that obvious compared with that on the piston TDC, the equivalent engine speed is limited within the range from 700 to 1500 rpm with the fuel mass changes from a wide range from −90% to 90%.

As the TDC of FPEs is required to be controlled within a tight limit [13,19,24,33], a TDC range from 14.5 mm to 18.5 mm with the corresponding injected fuel mass is enlarged and illustrated in Fig. 14. It is apparent that the TDC vs fuel profile is close to linear, with a linear approximation plot in the same picture as a comparison. Hence, the relation between the piston and the injected fuel amount per cycle can be further simplified and described by a linear equation in order to get the system transfer function.

4.2. PID feedback control

The Proportional-Integral-Derivative (PID) controller is a three-term controller that has a long history in the automatic control field. Due to its intuitiveness and its relative simplicity, in addition to satisfactory performance, it has become common practice to use the standard controller in industrial settings [34]. Applying a PID control law consists of properly applying the sum of three types of control actions: a proportional action, an integral action and a derivative one. These three actions can be described by the following equation [34]:

$$U(s) = \left(K_p + \frac{K_i}{s} + K_d s\right) E(s) \tag{19}$$

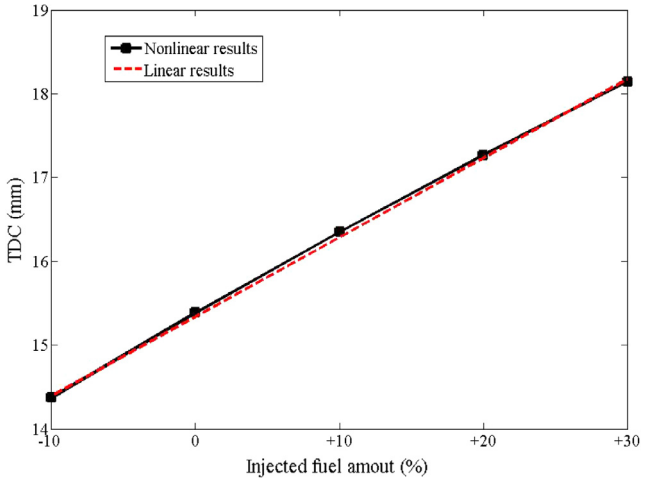

Fig. 14. Comparison with linear results.

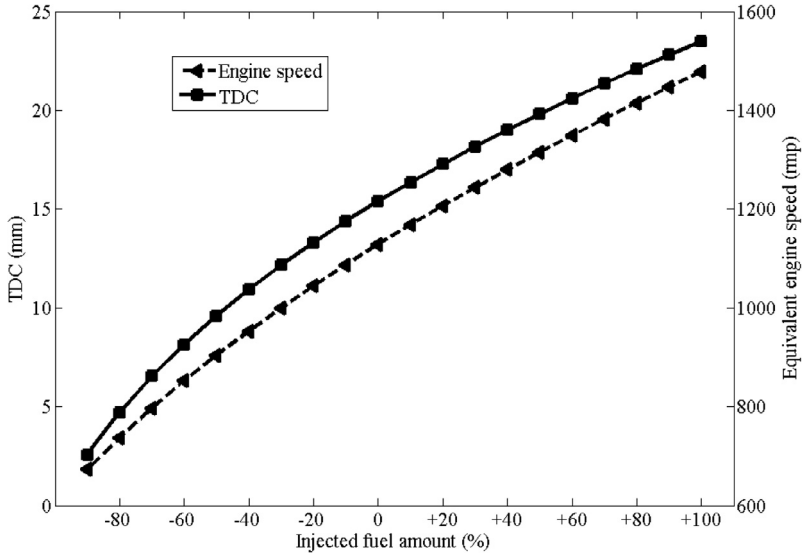

Fig. 13. Effects of injected fuel amount to TDC and engine speed.

The controller transfer function $C(s)$ can be written as:

$$C(s) = K_p + \frac{K_i}{s} + K_d s \tag{20}$$

where $U(s)$ is the control variable; $E(s)$ is the control error; K_p, K_i and K_d are the proportional gain, integral gain and derivative gain respectively.

Fig. 15 illustrates the FPEG plant coupled with a PID feedback controller, and it is a single-input single-output control loop. The target TDC is selected as the reference input for the control loop $R(s)$, with the actual piston TDC as the system output $Y(s)$. The control error $E(s)$ is the difference between the target TDC and its actual value, and is used as the input to the controller to calculate the fuel mass to the engine. As the system control variable, the fuel mass $U(s)$ will be updated by the controller in real time to reduce the control error.

From Fig. 14, the linear relationship between the output TDC $Y(s)$ and the injected fuel mass $U(s)$ can be described as:

$$Y(s) = C_3 U(s) \tag{21}$$

Then the transfer function of the FPEG system $G(s)$ is expressed as:

$$G(s) = C_3 \tag{22}$$

If the disturbance is ignored for now, then the closed-loop transfer function for the whole system can be derived as:

$$\frac{Y(s)}{R(s)} = \frac{C(s)G(s)}{1 + C(s)G(s)} \tag{23}$$

By substituting $C(s)$ and $G(s)$ from Eqs. (20) and (22), the closed-loop transfer function, from the reference input $R(s)$ to output $Y(s)$, is:

$$\frac{Y(s)}{R(s)} = \frac{C_3K_d s^2 + C_3K_p s + C_3K_i}{C_3K_d s^2 + (C_3K_p + 1)s + C_3K_i} \tag{24}$$

If a unit step input, $R(s) = \frac{1}{s}$ is applied to the system, the system steady-state response can be obtained by applying the final value theorem:

$$\lim_{t\to\infty} y(t) = \lim_{s\to 0} sY(s) = s \cdot \frac{C_3K_d s^2 + C_3K_p s + C_3K_i}{C_3K_d s^2 + (C_3K_p + 1)s + C_3K_i} \cdot \frac{1}{s} = 1 \tag{25}$$

This means for reference input of 1, the output is 1. There is no error at steady state, and the closed-loop control system tracks the input, which provides that the system is stable [35].

4.3. Controller performance analysis

As the effect of the derivative gain term is limited in the TDC control loop, the controller performance was investigated using a PI controller only [20]. By setting the values of the proportional gain and integral gain in the feedback control system, a PI controller was successfully implemented into the simulation. An example of the engine response to a 15% step decrease of electric load (the coefficient of the load force in Table 1 decreases from 700 to 595) is shown in Fig. 16. The disturbance occurs immediately at 1.0 s, and the controller performance is seen to

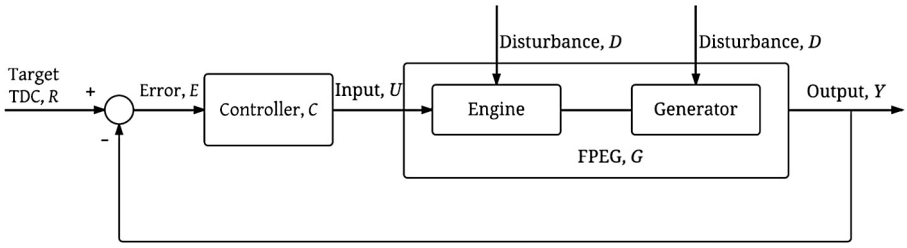

Fig. 15. PID feedback control system.

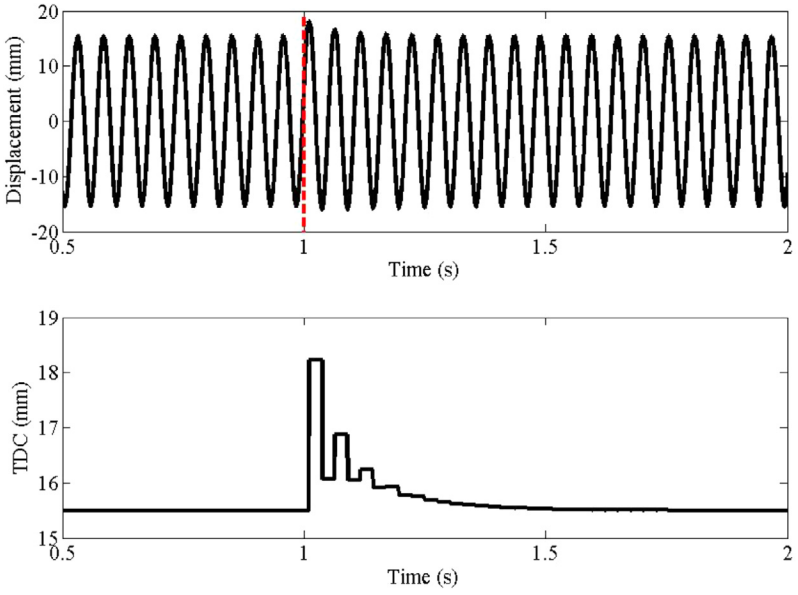

Fig. 16. PI Controller performance without variations.

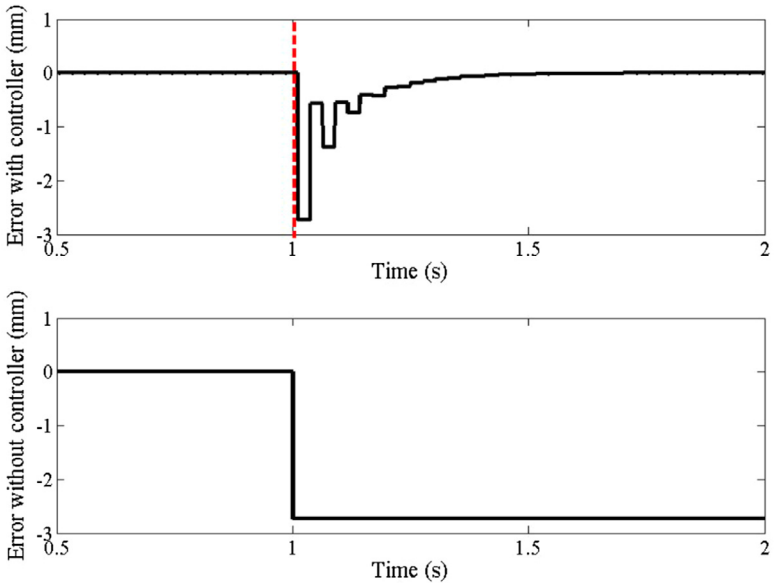

Fig. 17. Error analysis.

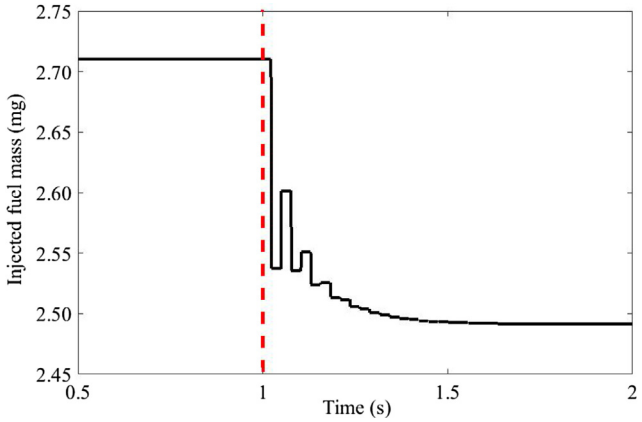

Fig. 18. The injected fuel mass for each cycle after the occurrence of the disturbance.

be satisfactory. The settling time is acceptable, and the piston TDC is controlled to back to the set point in 0.5 s.

The peak error, shown in Fig. 17, happens at the first cycle after the disturbance occurs. With the designed PI controller, the error begins to decrease from the second cycle, and then reduces to zero after several cycles. This is unavoidable as the controller is enabled to update the injected fuel mass only when an error is detected. The controller was manually tuned, and settling time could be further reduced by further optimised tuning process. In order to minimise the peak error and reduce the settling time, a predictive controller is suggested for the future research on the FPEG control strategy.

The injected fuel mass for each cycle after the occurrence of the disturbance is illustrated in Fig. 18. It is observed that the injector is controlled to take action from the next operation cycle to reduce the error. However, the variations on the injected fuel mass are presented in Fig. 18 are not that significant, which should be con-

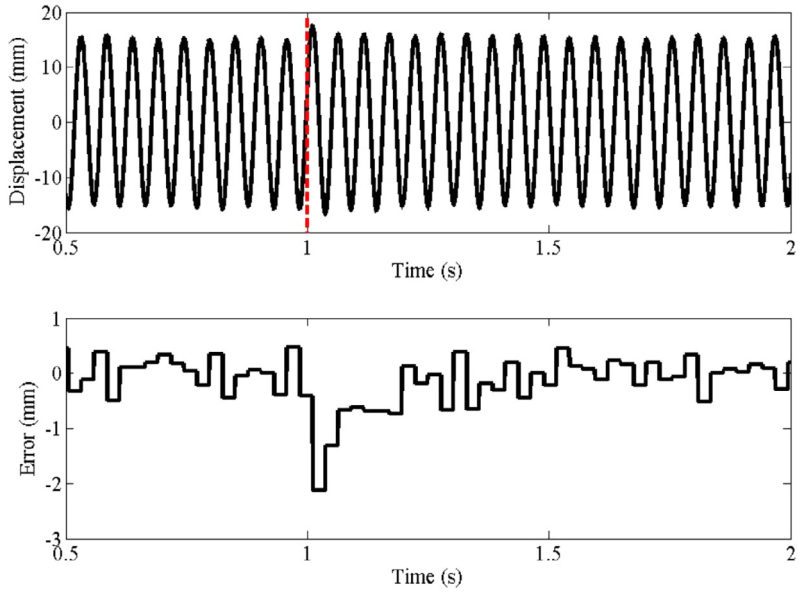

Fig. 19. Controller performance with variations.

trolled with high accuracy. The port injection system spray design means that the fuel is injected behind the intake valve, and the fuel will be draw into the cylinder when the intake valve opens. This may induce to some fuel drop out of the air, and may affect the control accuracy.

Fig. 19 shows an example of the controller performance after electric load step decreases along with cycle-to-cycle variations. Electric load change occurs immediately at 1.0 s by 15% and the error starts to reduce from the second cycle when the controller takes action. However, variations happens throughout the operation process, and cannot be eliminated. This is because the combustion efficiency η_c used to simulate the variations is a random value, and the burned fuel mass $U(s)\cdot\eta_c$ is then expressed by:

$$U(s)\cdot\eta_c = \left(K_p + \frac{K_i}{s} + K_d s\right)E(s)\cdot\eta_c \tag{26}$$

As a result, the cycle-to-cycle variation disturbance is simulated to occur after the controller calculation. The combustion efficiency is linked to a random value and by definition varies from cycle to cycle, hence the piston TDC is unable to remain constant by the controller with the current method.

5. Conclusion

This paper analysed the possible disturbances to the FPEG prototype using a fast-response numerical model. Immediate electric load change, engine cycle-to-cycle variations, and unsuccessful ignition are identified as three potential disturbances. During the engine operation, there could be one disturbance taking place or several disturbances take place simultaneously. From the simulation results, when step change of the electric load occurs, the corresponding change of piston TDC occurs in a step, and with different onset time, the TDC achieved during stable operation is the same. Low variations on piston TDC are observed when cycle-to-cycle variations take place. When unsuccessful ignition occurs, the engine will stop after one oscillation cycle. If the electric load changes along with engine misfire, with lower electric load, more oscillation cycles are observed for the engine to stop.

A PI feedback controller was implemented to the simulation to ensure the piston reached and maintained the target TDC when disturbance occurred. The injected fuel amount was selected as a potential control variable, with the target TDC as the reference input. The controller performance was seen to be satisfactory for the electric load step change. The settling time proved acceptable, and the piston TDC was controlled to back to the set point in 0.5 s. However, as cycle-to-cycle variation disturbance was simulated to occur after the controller calculation, the piston TDC is unable to remain constant by the controller with the current method.

Acknowledgements

This project was funded through the EPSRC grant EP/K503885/1. Data supporting this publication is openly available under an 'Open Data Commons Open Database License'. Additional metadata are available at: http://dx.doi.org/10.17634/123306-1. Please contact Newcastle Research Data Service at rdm@ncl.ac.uk for access instructions.

References

[1] Mikalsen R, Roskilly AP. The design and simulation of a two-stroke free-piston compression ignition engine for electrical power generation. Appl Therm Eng 2008;28(5):589–600. http://dx.doi.org/10.1016/j.applthermaleng.2007.04.009.
[2] Jia Boru, Zuo Zhengxing, Feng Huihua, Tian Guohong, Smallbone Andrew, Roskilly AP. Effect of closed-loop controlled resonance based mechanism to start free piston engine generator: simulation and test results. Appl Energy 2016;164:532–9. http://dx.doi.org/10.1016/j.apenergy.2015.11.105.
[3] Jia Boru, Zuo Zhengxing, Feng Huihua, Tian Guohong, Roskilly AP. Investigation of the starting process of free-piston engine generator by mechanical resonance. Energy Proc 2014;61:572–7. http://dx.doi.org/10.1016/j.egypro.2014.11.1173.
[4] Razali Hanipah M, Mikalsen R, Roskilly AP. Recent commercial free-piston engine developments for automotive applications. Appl Therm Eng 2015;75:493–503. http://dx.doi.org/10.1016/j.applthermaleng.2014.09.039.
[5] Erland Max. Fpec, free piston energy converter. In: Proceedings of the 21st electric vehicle symposium & exhibition. EVS; 2005.
[6] Jia Boru, Zuo Zhengxing, Feng Huihua, Tian Guohong, Roskilly AP. Development approach of a spark-ignited free-piston engine generator. SAE Technical Paper, 2014-01-2894; 2014 http://dx.doi.org/10.4271/2014-01-2894.
[7] Jia Boru, Zuo Zhengxing, Tian Guohong, Feng Huihua, Roskilly AP. Development and validation of a free-piston engine generator numerical model. Energy Convers Manage 2015;91:333–41. http://dx.doi.org/10.1016/j.enconman.2014.11.054.
[8] Mikalsen Rikard, Roskilly AP. A review of free-piston engine history and applications. Appl Therm Eng 2007;27(14):2339–52. http://dx.doi.org/10.1016/j.applthermaleng.2007.03.015.
[9] Zhang Shuanlu, Zhao Changlu, Zhao Zhenfeng. Stability analysis of hydraulic free piston engine. Appl Energy 2015;157:805–13.
[10] Johannes Haag, et al. Development approach for the investigation of homogeneous charge compression ignition in a free-piston engine. 2013, SAE Technical Paper, 2013-24-0047. http://dx.doi.org/10.4271/2013-24-0047.
[11] Li QF, Xiao Jin, Huang Zhen. Parametric study of a free piston linear alternator. Int J Automot Technol 2010;11(1):111–7. http://dx.doi.org/10.1007/s12239-010-0015-3.
[12] Kock Florian, Haag Johannes, Friedrich Horst E. The free piston linear generator-development of an innovative, compact, highly efficient range-extender module. SAE Technical Paper, 2013-01-1727; 2013. http://dx.doi.org/10.4271/2013-01-1727.
[13] Li Ke, Sadighi Ali, Sun Zongxuan. Active motion control of a hydraulic free piston engine. Mech IEEE/ASME Trans 2014;19(4):1148–59.
[14] Jia Boru, Smallbone Andrew, Zuo Zhengxing, Feng Huihua, Roskilly Anthony Paul. Design and simulation of a two-or four-stroke free-piston engine generator for range extender applications. Energy Convers Manage 2016;111:289–98. http://dx.doi.org/10.1016/j.enconman.2015.12.063.
[15] Feng Huihua, Guo Chendong, Yuan Chenheng, Guo Yuyao, Zuo Zhengxing, Roskilly Anthony Paul, et al. Research on combustion process of a free piston diesel linear generator. Appl Energy 2016;161:395–403. http://dx.doi.org/10.1016/j.apenergy.2015.10.069.
[16] Scott Goldsborough S, Van Blarigan Peter. A numerical study of a free piston ic engine operating on homogeneous charge compression ignition combustion. SAE Technical Paper, 1999-01-0619; 1999.
[17] Hibi A, Ito T. Fundamental test results of a hydraulic free piston internal combustion engine. Proc Inst Mech Eng Part D: J Automobile Eng 2004;218(10):1149–57.
[18] Mikalsen R, Roskilly AP. Performance simulation of a spark ignited free-piston engine generator. Appl Therm Eng 2008;28(14):1726–33.
[19] Mikalsen R, Roskilly AP. The control of a free-piston engine generator. Part 1: fundamental analyses. Appl Energy 2010;87(4):1273–80.
[20] Mikalsen R, Roskilly AP. The control of a free-piston engine generator. Part 2: engine dynamics and piston motion control. Appl Energy 2010;87(4):1281–7.
[21] Johansen Tor Arne, Egeland Olav, Johannessen Erling Aa, Kvamsdal Rolf. Free-piston diesel engine timing and control-toward electronic cam-and crankshaft. Control Syst Technol IEEE Trans 2002;10(2):177–90.
[22] Johansen Tor, Egeland Olav, Johannessen Erling Aa, Kvamsdal Rolf. Free-piston diesel engine dynamics and control. In: American control conference, proceedings of the 2001; 2001. IEEE.
[23] Johansen Tor A, Egeland Olav, Johannessen Erling Aa, Kvamsdal Rolf. Dynamics and control of a free-piston diesel engine. J Dyn Syst Meas Contr 2003;125(3):468–74.
[24] Jia Boru, Tian Guohong, Feng Huihua, Zuo Zhengxing, Roskilly AP. An experimental investigation into the starting process of free-piston engine generator. Appl Energy 2015;157:798–804. http://dx.doi.org/10.1016/j.apenergy.2015.02.065.
[25] Kosaka Hidemasa, Akita Tomoyuki, Moriya Kazunari, Goto Shigeaki, Hotta Yoshihiro, UmenoTakaji, Nakakita Kiyomi, Development of free piston engine linear generator system Part 1 – investigation of fundamental characteristics. SAE Technical Paper, 2014-01-1203; 2014.
[26] Goto Shigeaki, Moriya Kaznunari, Kosaka Hidemasa, Akita Tomoyuki, Hotta Yoshihiro, Umeno Takaji, Nakakita Kiyomi, Development of free piston engine linear generator system Part 2 – investigation of control system for generator. SAE Technical Paper, 2014-01-1193;2014.
[27] Hanipah Mohd Razali. Development of a spark ignition free-piston engine generator. Dissertation, Newcastle University; 2015.
[28] Jia Boru, Smallbone Andrew, Feng Huihua, Tian Guohong, Zuo Zhengxing, Roskilly AP. A fast response free-piston engine generator numerical model for control applications. Appl Energy 2016;162:321–9. http://dx.doi.org/10.1016/j.apenergy.2015.10.108.

[29] Harris Cyril M, Piersol Allan G, Paez Thomas L. Harris' shock and vibration handbook, vol. 5. New York: McGraw-Hill; 2002.
[30] Feng Huihua, Guo Chendong, Jia Boru, Zuo Zhengxing, Guo Yuyao, Roskilly Tony. Research on the intermediate process of a free-piston linear generator from cold start-up to stable operation: Numerical model and experimental results. Energy Convers Manage 2016;122:153–64. http://dx.doi.org/10.1016/j.enconman.2016.05.068.
[31] Miao Yuxi, Zuo Zhengxing, Feng Huihua, Chendong Guo Yu, Song Boru Jia, Guo Yuyao. Research on the combustion characteristics of a free-piston gasoline engine linear generator during the stable generating process. Energies 2016;9(8):655. http://dx.doi.org/10.3390/en9080655.
[32] Jia Boru, Mikalsen Rikard, Smallbone Andrew, Zuo Zhengxing, Feng Huihua, Roskilly Anthony Paul. Piston motion control of a free-piston engine generator: a new approach using cascade control. Appl Energy 2016;179:1166–75. http://dx.doi.org/10.1016/j.apenergy.2016.07.081.
[33] Mikalsen R, Jones E, Roskilly AP. Predictive piston motion control in a free-piston internal combustion engine. Appl Energy 2010;87(5):1722–8.
[34] Ang Kiam Heong, Chong Gregory, Li Yun. Pid control system analysis, design, and technology. Control Syst Technol, IEEE Trans 2005;13(4):559–76.
[35] Roskilly Tony, Mikalsen Rikard. Marine systems identification, modeling and control. Butterworth-Heinemann; 2015.